

Alternative technology towards clean and sustainable industry: Conversion of carbon dioxide emission gas into potassium carbonate

Nuryoto Nuryoto^{1*}, Muhammad Harsya Alfarizi¹,
Muhamad Adam Surya Kelana¹, Rafif Nur Tahta Bagaskara²

¹ Chemical Engineering Department, Faculty of Engineering, Universitas Sultan Ageng Tirtayasa, Jl. Jendral Sudirman KM. 3, Cilegon, Banten, 42435, Indonesia

² School of Environment, Faculty of Arts and Science, University of Toronto, 33 Willcocks Street, Suite 1016V, Toronto, ON, M5S 3E8, Canada

* Corresponding author's e-mail: nuryoto@untirta.ac.id

ABSTRACT

The increase in carbon dioxide (CO₂) gas emissions by more than 50% between 2000 and 2023 from industrial processes has triggered an increase in greenhouse gases and global warming. Effective, efficient, and economical CO₂ capture that can be integrated with existing processes to maintain environmental stability is greatly needed. The integration of influential factors in the absorption and diffusion-reaction processes must be well-combined to achieve the desired operating conditions. The research aims to analyze the occurring phenomena and determine the amount of K₂CO₃ product generated from the CO₂ capture process by integrating influential factors, namely KOH concentration, reaction temperature, and stirring speed. Observations were conducted at 9800 Pa pressure, KOH solution concentration of 6–8 M, stirring speed of 200–300 rpm, reaction temperature of 30–50 °C, CO₂ flow rate of 2 dm³/minute, and reaction time of 150 minutes. The CO₂ capture results were analyzed using gravimetric and instrumentation methods to evaluate the products. Observation results showed that the best conditions were obtained at 8 M KOH concentration, 300 rpm stirring speed, and 50 °C reaction temperature, with KOH conversion reaching 53.43% and K₂CO₃ product of 54.94 grams. These results indicate that integrating influential factors in the absorption and diffusion-reaction processes positively impacts CO₂ capture. However, the process is not optimal, as the KOH conversion is still far below 100%. Therefore, further research must be conducted by combining the previously studied influential factors such as reaction time, CO₂ gas flow rate, and CO₂ gas distributor holes to maximize KOH conversion and K₂CO₃ product yield.

Keywords: diffusivity, chemical reaction, reaction rate constant, greenhouse effect, carbon dioxide capture.

INTRODUCTION

Carbon dioxide (CO₂) is a compound that triggers climate change and global warming [1, 2], which leads to greenhouse effects, ocean acidification, and chemical imbalances in Earth's atmosphere [3]. CO₂ comes from human activities, primarily production processes [4]. In 2000, the industry produced CO₂ emissions of 25.51 billion tons, which increased by more than 50% to 37.79 billion tons in 2023 [5]. This condition is quite concerning, so anticipatory actions need to be

taken, one of which is processing CO₂ emission gas before releasing it into the environment. CO₂ transformation through an absorption process integrated with a reaction process, namely using an alkaline solution in the form of KOH, can be used as an alternative step to solve this problem. The high solubility of KOH and good dissociation in water [6] allows CO₂ gas dissolved in KOH solution to easily interact with K⁺ and OH⁻ ions to react, forming potassium carbonate product (see Figure 1). When CO₂ gas transforms into potassium carbonate product, the economic value of

CO₂ emission gas will increase. The potassium carbonate product generated from CO₂ capture can be used as a catalyst [7], food additive [8], and raw material for the ceramic industry [9].

Conventionally, potassium carbonate is produced from the Solvay process [10] and can also be produced through an electrochemical process. The Solvay process potentially requires high energy input and significant costs due to heating and separation processes and involves multiple raw materials, namely NaCl, CaCO₃, and KOH [11]. While the electrochemical process potentially yields more effective potassium carbonate production than the Solvay process, it requires advanced technology and expertise, thus necessitating a substantial initial investment. Based on these considerations, this research attempts to conduct observations using a different method, namely the carbonation method, where CO₂ gas is contacted with a potassium hydroxide (KOH) solution. The use of the carbonation method has two advantages: first, it is more cost-effective as it only involves two reactants, namely CO₂ gas and KOH, and second, it contributes to maintaining CO₂ level stability in the atmosphere as it can be integrated with existing processes such as power plant chimney outputs and boilers which are sources of CO₂ emissions.

Based on the literature review conducted, previous research has primarily focused on how much CO₂ can be captured in KOH solution (see Table 1) and has not yet focused on how and how much K₂CO₃ product can be produced from the contact process between the two (CO₂ and KOH). Looking at Table 1, it appears that the capture of CO₂ into KOH is still relatively low, with the highest only able to absorb 800 mg of CO₂ gas/gram of KOH absorbent [12]. To address the problem of low CO₂ capture, combination of factors affecting this process is needed to maximize the interaction between CO₂ and KOH.

Theoretically, CO₂ capture is directly influenced by the pressure in the processing system (see Equation 1) [13].

$$y_{CO_2}P = H_{CO_2-H_2O} \cdot x_{CO_2} \quad (1)$$

where: y_{CO_2} – molar fraction of CO₂ in gas phase (dimensionless), x_{CO_2} – molar fraction of CO₂ in liquid phase (dimensionless), and $H_{CO_2-H_2O}$ – Henry constant CO₂ – H₂O (Pa), P– system pressure (Pa).

Thus, when the system is pressurized (P), the amount of CO₂ dissolved in water (x_{CO_2}) will be more significant compared to without pressure (atmospheric) [14]. The steps taken by previous researchers who conducted the process in a pressurized system were very appropriate. The low CO₂ capture in previous studies was likely due to the diffusion-reaction process running less than optimally, and the CO₂ absorbed by water could be rereleased when CO₂ did not interact well with KOH to react and form the K₂CO₃ product.

Referring to the low CO₂ capture results (see Table 1), this research aims to integrate factors that influence the diffusion-reaction process to maximize CO₂ capture and reaction product (K₂CO₃) by integrating variables of stirring speed, reaction temperature, and KOH concentration (absorbent). On the diffusion side, stirring performed in the processing system will reduce the film layer (z) [19], and the process system temperature will increase the diffusivity coefficient (D) [20]; thus, the effect will increase the diffusion rate (J_{CO_2}) or molecular mass transfer of CO₂ into the KOH solution. On the reaction side, referring to the Arrhenius equation, increasing temperature will increase the reaction rate constant (k_1) [21], and increasing KOH concentration in the process system will increase the value of C_{KOH} . Therefore, integrating these three variables (temperature, stirring, and KOH concentration) is expected to positively impact the diffusion rate and reaction rate that occurs in

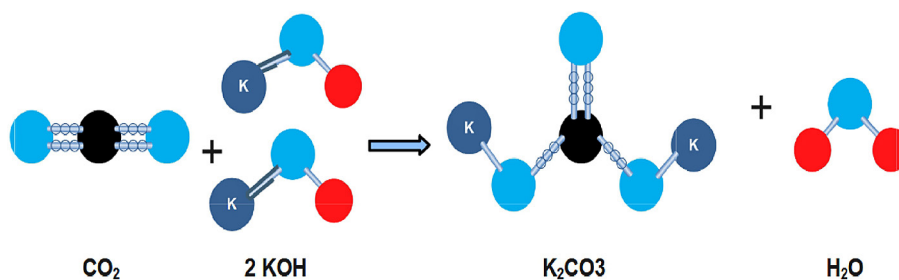


Figure 1. Illustration of the reaction process between CO₂ and KOH to form K₂CO₃

Table 1. CO₂ capture using KOH solution

No.	Raw materials	Operational Condition	Research results	References
1	KOH and CO ₂ with 99.9% purity.	Reaction temperature 25–65 °C, pressure 2–10 bar, KOH: 0.5–25 grams, and using batch reactor.	The optimum temperature was obtained at 45 °C, with an adsorbent amount of 0.5 grams and the highest absorption rate of 800 mg CO ₂ /g KOH absorbent. The amount of K ₂ CO ₃ product is not known.	[12]
2	KOH, activated carbon in the form of Polyacrylonitrile (PAN), and CO ₂ with 99.9% purity.	The activated carbon pretreatment process was carried out at 800 °C, followed by activation using OH (weight ratios 1:1 to 4:1), activation temperatures 600–900 °C.	Maximum CO ₂ adsorbed was 2.5 mmol/g, achieved at a temperature of 30 °C with a KOH: PAN ratio of 3:1, with no information on the amount of K ₂ CO ₃ product.	[15]
3	KOH and CO ₂ .	KOH concentration variations of 1–5 N/50 ml distilled water, room temperature, and atmospheric pressure.	The highest absorption was obtained at 1 N KOH, which was 0.3750 mol CO ₂ /mol KOH.	[16]
4	KOH and CO ₂ .	CO ₂ concentration 3–15% with CO ₂ flow rate 400–2000 cm ³ /min, process temperature 10–50 °C, KOH concentration 30–190 g/dm ³ , and pressure: 1–5 bar.	Maximum CO ₂ absorption of 0.76 g CO ₂ /g KOH was obtained at a CO ₂ concentration of 15% and pressure of 5 bar. No information is available on the K ₂ CO ₃ product.	[17]
5	KOH and CO ₂ .	Absorption temperature 25–65 °C, pressure 2–10 bar, and KOH concentration 0.01–1.21 mol/ dm ³ .	Optimal conditions were achieved at a temperature of 35 °C, pressure of 4 bar, and KOH concentration of 0.412 mol/ dm ³ , with a CO ₂ removal efficiency of 32.22%.	[18]

the CO₂-KOH system. Thus, this research aims to analyze the occurring phenomena and determine how much K₂CO₃ product is produced from the CO₂ capture process by integrating influential factors, namely KOH concentration, reaction temperature, and stirring speed.

Figure 2 describes the reaction illustration in Figure 1 in detail. When CO₂ gas is

introduced into the KOH solution, the CO₂ gas bubbles into the solution. After the interaction between CO₂ and KOH occurs, they react to form potassium carbonate (K₂CO₃) and water (H₂O). When the diffusion-reaction process in the system has reached steady-state conditions, the diffusion rate will be equal to the reaction rate (see Equations 2–5).

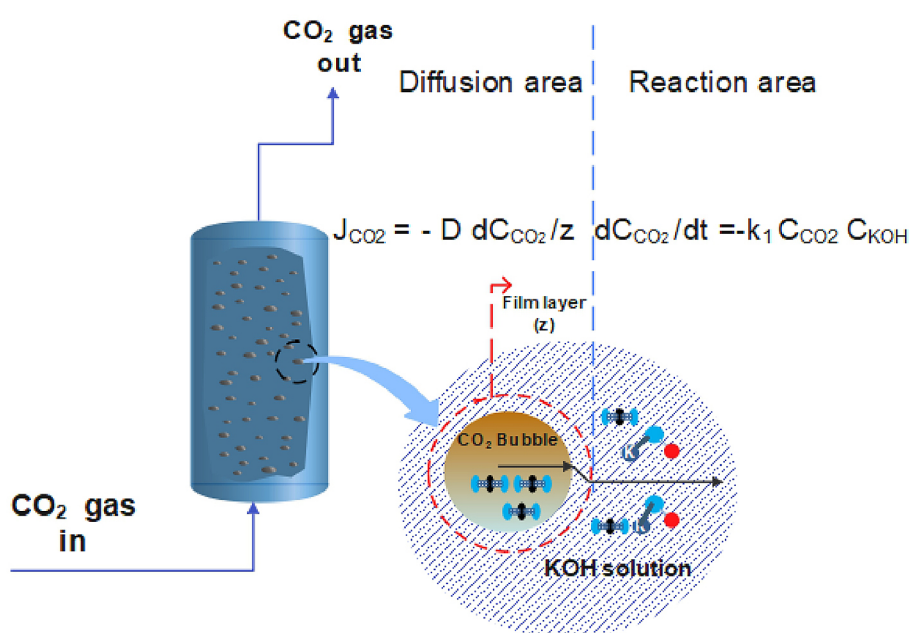


Figure 2. Diffusion-reaction process in K₂CO₃ synthesis using CO₂ gas and KOH

$$J_{CO_2} = -D \frac{dC_{CO_2}}{z} \quad (2)$$

$$\frac{dC_{CO_2}}{dt} = -k_1 C_{CO_2} C_{KOH} \quad (3)$$

$$J_{CO_2} = -D \frac{dC_{CO_2}}{z} \approx \frac{dC_{CO_2}}{dt} = k_c (C_{CO_2b} - C_{CO_2}) \quad (4)$$

$$k_c (C_{CO_2b} - C_{CO_2}) = -k_1 C_{CO_2} C_{KOH} \quad (5)$$

where: J_{CO_2} – CO₂ molecular flux (mol/dm²·s),
 D – diffusion coefficient (dm²/s),
 C_{CO_2b} – CO₂ concentration in bubble (mol/dm³),
 C_{CO_2} – CO₂ concentration in solution (mol/dm³),
 C_{KOH} – concentration of KOH (mol/dm³),
 z – film layer (dm),
 $D \frac{dC_{CO_2}}{dz}$ – concentration gradient (mol/dm⁴),
 $\frac{dC_{CO_2}}{dt}$ – rate of concentration change (mol/dm³·s),
 k_c – mass transfer coefficient (dm/s),
 k_1 – reaction rate constant (dm³/mol·s).

The results obtained from this research are expected to complement existing research information and provide insights into the impacts of the integration implemented (temperature, KOH concentration, and stirring speed) on the amount of K₂CO₃ product produced, whether it has positive or negative effects on the diffusion-reaction system. Additionally, it can contribute to the scientific and technological advancement.

MATERIALS AND METHODS

Materials and research equipment

The raw materials used were CO₂ gas with 99.9% purity obtained from CV. Purnama Jaya Gas, Cilegon, Banten, Indonesia. KOH Merck purchased from Shopee Indonesia marketplace was dissolved in distilled water to form a KOH solution with KOH concentrations of 6, 7, and 8 molarity (M). The research equipment used in this study consisted of: (1) CO₂ gas cylinder, (2) gas regulator, (3) flow meter, (4) overhead magnetic stirrer, (5) heating mantle, (6) three-holes gas distributor, (7) three-neck flask, (8) thermometer, and (9) water tank. Equipment details are illustrated in Figure 3.

Experimental procedure

Water was added to the water tank to a height of 100 cm (equivalent to 9800 Pa hydrostatic pressure). KOH solution with specific concentrations (6, 7, and 8 M) was placed into the three-neck flask, and then the stirrer was operated at predetermined speeds of 200 and 300 rpm. The heating mantle was switched on, and the operating temperature was set according to the reaction temperature (30, 40, and 50 °C). When all parameters were reached, the CO₂ gas regulator was opened to flow CO₂ gas into the KOH solution at a flow rate of 2 dm³/minute. The reaction

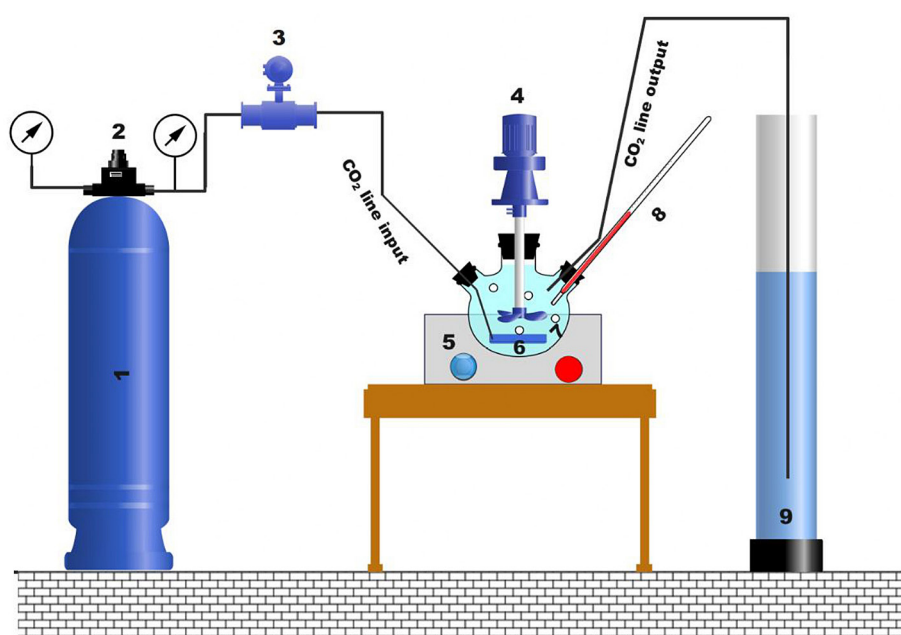


Figure 3. Illustration of K₂CO₃ synthesis research equipment.

time was stopped after 150 minutes. The reaction product was separated from the liquid using filter paper. The filtered product was dried in an oven at 110 °C for 2 hours to evaporate the remaining water. The amount of product produced was calculated using Equation 6.

$$W_{K_2CO_3} = w_0 - w_1 \quad (6)$$

where: $W_{K_2CO_3}$ – mass of K_2CO_3 produced (grams), w_0 – mass of product + filter paper after oven drying (grams), w_1 – mass of empty filter paper (grams).

To further understand the phenomena, this research attempted to model the occurring reaction process using a mathematical model in the form of reaction kinetics, which was conducted under optimal operating conditions. For this purpose, data on the decrease in KOH concentration over reaction time was obtained from sample analysis using the acid-base titration method with 0.1 N HCl titrant. To ensure the accuracy and consistency of data, particularly for mathematical model calculations, the titration process was conducted 3 times, and the data was subsequently averaged. The KOH content from titration was calculated using Equation 7.

$$C_{KOH} = \frac{Vt.N.Mw}{Vs} \quad (7)$$

where: C_{KOH} – KOH concentration at a specific time (mg/dm³), Vt – titrant volume (dm³), N – HCl titrant normality (N), Mw – molecular weight (grams/mol), Vs – sample volume (dm³).

Determining parameters or observation variables in this research referred to the best results from previous studies. The KOH concentration variable in the 6–8 M range was based on CO₂ capture research using eutectic solvents, which yielded satisfactory results [22]. The stirring speeds of 200 and 300 rpm were selected based on the transformation of CO₂ into Precipitated Calcium Carbonate (PCC) using Ca(OH)₂, which produced optimal products [23]. The reaction temperature of 30–50 °C was adopted from relevant research on CO₂ capture [12, 18], which yielded satisfactory results, and the reaction system pressure of 9800 Pa and CO₂ gas flow rate of 2 dm³/minute was set according to the best conditions in PCC synthesis [23]. The drying temperature, which was set to 110 °C for 2 hours, was chosen based on research that produced optimal drying results [23]. By integrating the best parameters from previous

research, the absorption and diffusion-reaction processes are expected to run optimally, and the resulting K₂CO₃ will be maximized.

To achieve the highest yield of K₂CO₃, CO₂ capture equipment typically uses a KOH solution as an absorbent in an absorber column. However, this research employs a different approach. The method implemented involves modification through a bubble reaction concept, utilizing a stirred semi-batch bubble reactor (Figure 3). This setup allows maximum interaction between CO₂ bubbles and the KOH solution, optimizing the diffusion-reaction process.

Characterization techniques

On the dried reaction products, characterization was performed through testing using instrumentation equipment in fourier transform infrared spectroscopy (FTIR) type Alpha II Bruker – ATR Germany to analyze its function group peaks and compare them with existing reference standards. This action was taken to ensure that the K₂CO₃ product was formed. Scanning electron microscopy (SEM) testing using Zeiss – Germany was conducted to observe morphological changes and reinforce the FTIR test results.

Mathematical model testing

The mathematical model used in this research was a simple mathematical model, namely the pseudohomogeneous reaction kinetics model (referring to Equation 8). Several assumptions were used, including that CO₂ was continuously input and stopped when the reaction time ended, so it was assumed that CO₂ was in excess. The reaction in the reverse direction was ignored. The concentration measurement was in the KOH; therefore, the mathematical model calculation approach was based on changes in KOH concentration during the reaction process. Referring to these assumptions, Equation 8 was modified and simplified to become Equation 9.

$$-\frac{dC_{CO_2}}{dt} = k_1 C_{CO_2} C_{KOH} - k_2 C_{H_2O} C_{K_2CO_3} \quad (8)$$

$$-\frac{dC_{CO_2}}{dt} = k_1 C_{CO_2} C_{KOH} \quad (9)$$

Equation 9 is identical to Equation 3 and is subsequently modified to become Equation 10.

$$-\frac{dC_{KOH}}{dt} = k_1' C_{KOH} \quad (10)$$

where: $k_1' = k_1 C_{CO_2}$

Equation 10 can be modified into a second-order equation, becoming Equation 11.

$$-\frac{dC_{KOH}}{dt} = k_1' C_{KOH}^2 \quad (11)$$

Therefore, the models to be developed are first-order (Equation 10) and second-order (Equation 11). Lastly, they are integrated to obtain Equations 12 and 13.

$$\ln C_{KOH} = \ln C_{KOH_0} + k_1' t \quad (12)$$

$$\frac{1}{C_{KOH}} = \frac{1}{C_{KOH_0}} + k_1' t \quad (13)$$

The k_1' value will be obtained using Microsoft Excel and creating trendlines for $\ln C_{KOH}$ versus t (first-order) and $\frac{1}{C_{KOH}}$ versus t (second-order). A mathematical model that has an R^2 value (coefficient of determination) approaching 1 indicates that the mathematical model is valid and can be used to describe the phenomenon of the reaction process that occurs and predict conversion under other operating conditions, as well as being applicable for reactor design in the future.

RESULTS AND DISCUSSION

Effect of KOH concentration

As shown in Figure 4, increasing KOH concentration leads to an increase in the produced potassium carbonate (K_2CO_3), with KOH concentrations of 6, 7, and 8 M yielding K_2CO_3 products of 21.01, 30.43, and 36.64 grams, respectively. Using the K_2CO_3 product of 21.01 grams as the baseline, there was an increase of 44.84% in K_2CO_3 product quantity from 21.01 grams to 30.43 grams and 80.30% from 21.01 grams to 36.64 grams. This data shows that the increase in KOH concentration significantly impacts CO_2 absorption. This phenomenon aligns with Equation

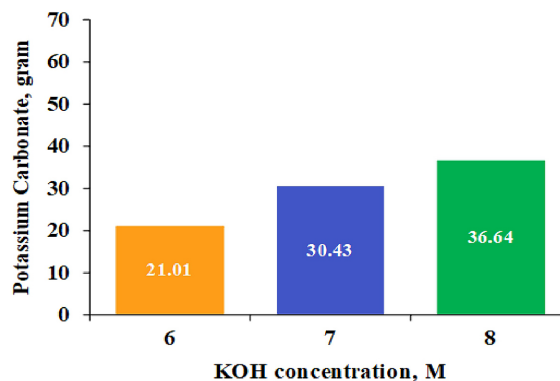


Figure 4. Effect of KOH concentration on K_2CO_3 product at 200 rpm and reaction temperature of $30^\circ C$

5 because increasing the adsorbent concentration enhances gas-liquid molecular interactions, increasing the diffusion and reaction rates [24].

Referring to Equation 5 and the results obtained in Figure 4, increasing KOH concentration above 8 M could achieve maximum CO_2 capture and optimal K_2CO_3 product yield. Although naturally, too high of a KOH concentration increase in the gas-liquid reaction system will create a new barrier, namely an increase in KOH solution viscosity [25], thus reducing CO_2 gas diffusion into the KOH solution, and will affect the chemical reaction rate between CO_2 gas and KOH. However, since stirring was performed in the diffusion-reaction system, the barriers that arise from viscosity effects on diffusion-reaction can be eliminated.

The trend observed in this research (in Figure 4) also occurs in syngas synthesis with CO_2 , CH_4 , and H_2O reactants from existing references [26]; although the research conducted was different, the concept is the same. When the concentration of methane (CH_4) reactant is increased, and the CH_4/CO_2 ratio increases from 0.538 to 3.03, the syngas product produced, mainly hydrogen (H_2), also increases from about 31% to 39% [26]. Other research shows similar trends to this study (see Table 2). As shown in Table 2, increasing absorbent concentration positively impacts CO_2 capture.

Table 2. Effect of absorbent concentration on CO_2 capture

Range of absorbent concentration	% reactant conversion, product mass, or % removal	References
Monoethanolamine (MEA) concentration: 15–40%	CO_2 removal percentage increased from approximately 54% to 93%	[27]
Monoethanolamine (MEA) concentration: 10–30%	CO_2 removal percentage increased from approximately 34% to 76%	[28]
KOH concentration: 6, 7, and 8 M	The increase in CO_2 capture is marked by an increase in K_2CO_3 yield, which is from 21.01 to 30.43 and 36.64 grams, respectively.	This research

Effect of stirring speed

The increased stirring speed positively impacted the amount of potassium carbonate product produced (see Figure 5), with the potassium carbonate product increasing from 36.64 grams to 41.26 grams (an increase of 12.61%). A similar phenomenon to this research also occurred in other studies (see Table 3), where increase stirring speed positively impacted process performance.

The results in Table 3 prove that increasing the stirring speed in this study reduced diffusivity barriers in the form of film layers (see Figure 2 and Equation 2). Increased stirring will reduce the

film layer and interphase contact, increasing the mass transfer coefficient from the gas to the liquid phase [31]. Other impacts include increased interaction with CO₂ gas nuclei, increased velocity and shear stress of each fluid, creation of micro mixing, and maximum molecular interaction between the gas-liquid fluid system, allowing the reaction process to proceed optimally [32, 33].

Based on the visual observation in Figure 5, no vortex has occurred at a stirring speed of 300 rpm yet, so there is potential to increase the speed above 300 rpm to its maximum stirring speed to produce even more K₂CO₃ product. The maximum allowable stirring speed is before a vortex

Table 3. Effect of stirring speed on reaction process performance and waste degradation

Stirring speed (rpm)	% reactant conversion, product mass, or % removal	References
100–400	The sugar waste removal percentage increased from 71% to 83.4%	[29]
200–500	The rapeseed oil conversion increased from approximately 41% to 71%	[30]
200 and 300	K ₂ CO ₃ product increased from 36.64 grams to 41.26 grams	This research

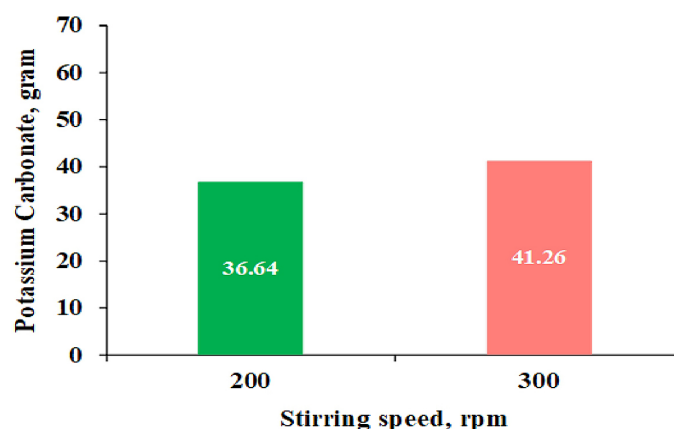


Figure 5. Effect of stirring speed on K₂CO₃ product at KOH concentration 8 M and reaction temperature of 30 °C

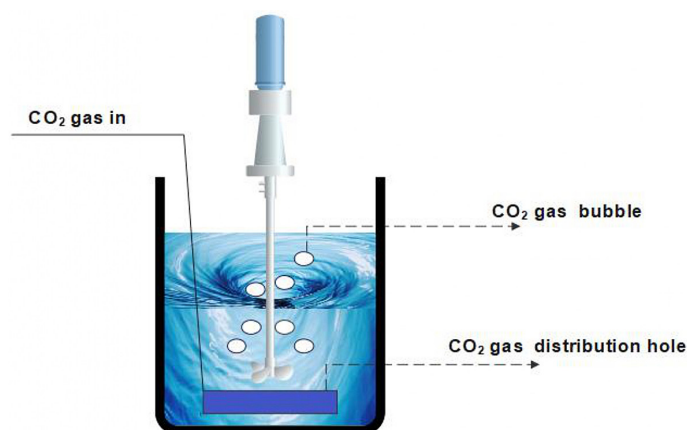


Figure 6. Illustration of vortex phenomenon in CO₂ gas-liquid absorbate reaction process

forms, creating a whirlpool current, as shown in Figure 6. When this condition occurs, CO₂ gas bubbles escape through the vortex before contacting the KOH solution.

The vortex phenomenon, as shown in Figure 6, was experienced in research on converting CO₂ gas into Precipitated Calcium Carbonate (PCC) [23]. When the stirring speed was increased from 400 to 500 rpm, excessive vortexing occurred (forming a whirlpool), and CO₂ gas bubbles were observed escaping through this whirlpool, causing the PCC product yield to decrease from 7.64 grams (at stirring speed of 400 rpm) to 6.55 grams (at stirring speed of 500 rpm).

Effect of reaction temperature

The increase in reaction temperature increased the amount of K₂CO₃ produced (Figure 7). As shown in Figure 7, the products obtained at reaction temperatures of 30, 40 and 50 °C were 41.26, 45.33, and 54.94 grams, respectively. When calculated as percentages with the baseline at 30°C, there was an increase of 9.86% from 30 to 40 °C and 33.16% from 30 to 50 °C.

A similar phenomenon was also observed in investigations conducted on biodiesel synthesis [34], where increasing the reaction temperature from 150 to 180 °C significantly increased triglyceride conversion to biodiesel [34].

The research data and reference [34] show that the reaction temperature factor significantly enhances the reaction process. Referring to the Arrhenius equation (Equation 14), as previously explained, an increase in reaction temperature will cause an increase in the reaction rate constant (*k*₁).

$$k_1 = A e^{-\frac{E_a}{RT}} \tag{14}$$

where: *k*₁ – reaction rate constant (units depend on reaction order), A – frequency factor (units depend on reaction order), E_a – activation energy (J/mol), R – universal gas constant (8.314 J/mol. K), T – absolute temperature (K).

Other research results showed a similar trend, where increasing the liquid temperature increased CO₂ capture (Table 4).

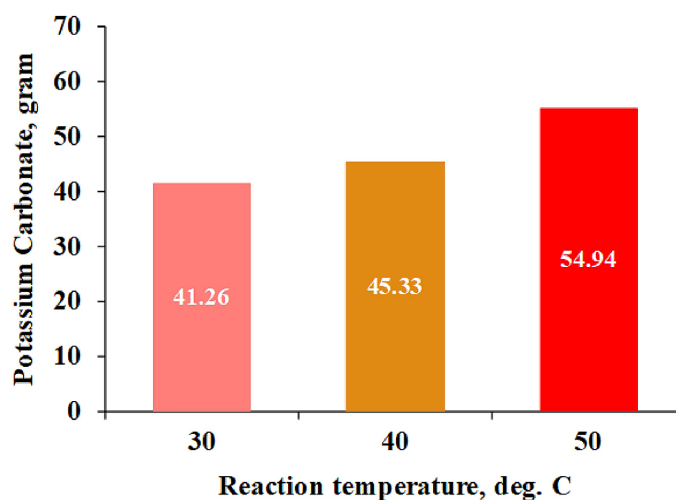


Figure 7. Effect of reaction temperature on K₂CO₃ product at KOH concentration of 8 M and stirring speed of 300 rpm

Table 4. Effect of temperature on CO₂ capture

Temperature range (°C)	% reactant conversion, product mass, or % removal	References
Absorbent: Monoethanolamine (MEA); temperature: 20.9 and 39.5 °C	CO ₂ capture increased to 81% at 20.9 °C and 95%	[35]
Absorbent: biphasic; temperature: 30 and 60 °C	CO ₂ capture increased from 6% to 12% when the temperature was raised from 30 to 60 °C	[36]
Absorbent: KOH solution; temperature: 30 to 50 °C	CO ₂ capture increased as evidenced by the K ₂ CO ₃ produced, which increased from 41.26, 45.33, and 54.94 grams for 30, 40, and 55 °C system temperatures, respectively	This research

However, increasing the system temperature in gas-liquid reactions at specific temperatures can decrease the reaction rate. This phenomenon occurred when the system temperature increase exceeds its maximum point, resulting in reduced solubility CO₂ gas in the KOH solution. Observations of H₂ gas solubility in water show that at 298 K, the solubility of H₂ (x_{H_2}) was 0.00135994, and when the temperature increased to 323.50 K, H₂ solubility decreased to 0.00123925 [37]. Therefore, increasing the reaction system temperature must be done carefully in gas-liquid reaction systems, as it can have positively and negatively affects the reaction rate.

Based on the observations, increasing the KOH concentration from 6 to 8 M, along with stirring speeds of 200 and 300 rpm and reaction temperatures between 30 °C and 50 °C, generally led to an increase in CO₂ capture, as indicated by the higher yield of K₂CO₃. This phenomenon can be explained in more detail by connecting it with the diffusion-reaction concept presented in Equations 2 to 5 and relating it to Equations 15 to 17 [38, 39].

$$Sh = \frac{k_c dp}{D} \quad (15)$$

$$Sh = 2 + 0.553 Re^{0.5} Sc^{0.33} \quad (16)$$

$$Re = \frac{\rho N dp^2}{\mu} \quad (17)$$

where: *Sh* – Sherwood number (dimensionless), *dp* – CO₂ bubble diameter (m), *N* – stirring speed (rps), *m* – adsorbent mass (gram), μ – viscosity (kg/m·s), *Re* – Reynolds number (dimensionless), *Sc* – Schmidt number (dimensionless).

Referring to Equations 15 to 17, increasing the stirring speed, without causing vortex formation (as illustrated in Figure 6), will enhance the Reynolds number, Sherwood number, and mass transfer coefficient (*k_c*). This, in turn, leads to a higher diffusivity rate and subsequently increases the reaction rate between CO₂ and KOH (refer to Equations 4 to 5). On the other hand, increasing KOH concentration will increase solution viscosity, which affects the mass transfer coefficient (*k_c*) (referring to Equations (15) to (17)). However, in this study, the stirring process could potentially eliminate the impact of increased KOH concentration on the reduction of mass transfer coefficient (*k_c*) for CO₂ gas. This hypothesis is supported by reaction results showing that increased KOH concentration can increase K₂CO₃ product (see Figure 4). According to Equation (17), the

stirring speed (*N*) is proportional to the increase in Reynolds number. On the other hand, the increase in viscosity due to higher KOH concentration is inversely proportional, which can lead to a decrease in the Reynolds number. When the effect of the increased stirring speed outweighs the increase in viscosity, the Reynolds number will rise. Under these conditions, the interaction between CO₂ and KOH in the system, which involves the diffusion-reaction process, will also intensify, leading to a greater production of the reaction product (K₂CO₃). Based on theoretical reasoning and observed phenomena, it is likely correct to assume that the reduced mass transfer due to increased viscosity can be counterbalanced by raising the stirring speed. Furthermore, an increase in KOH concentration will impact the rate of the chemical reaction. According to Equation (3), the reaction rate is dependent on the KOH concentration (*C_{KOH}*). Therefore, as the concentration of KOH rises, the reaction rate will also increase. It is essential to ensure that the diffusion-reaction process operates optimally so that the resulting products meet the desired targets. The temperature of the KOH solution used in CO₂ capture influences both the diffusion and reaction process. During the reaction process, an increase in system temperature raises the reaction rate constant (*k₁*), as described by the Arrhenius equation (Equation (14)). On the other hand, in the diffusion process, higher system temperatures reduce the viscosity of the KOH solution. This decrease in viscosity results in a higher Reynolds number, which subsequently leads to an increase in the mass transfer coefficient (*k_c*). Therefore, the results obtained in this study, which showed an increase in K₂CO₃, are logical. However, all parameters certainly have their optimal point. If we refer to CO₂ capture observations conducted using 2-(1-piperazinyl) ethylamine sarcosinate as an absorbent at temperatures of 57 to 77 °C, where CO₂ capture decreased when the temperature was raised above 67 °C [40]. Future research should investigate temperatures above 50 °C. This approach will help validate this phenomenon and determine whether different absorbents exhibit similar trends, as each compound has its own unique characteristics.

When examining the reaction product at a temperature of 50 °C, with a KOH concentration of 8 M and a stirring speed of 300 rpm (as shown in Figure 8), we observed that the optimal operating conditions in this study resulted in the

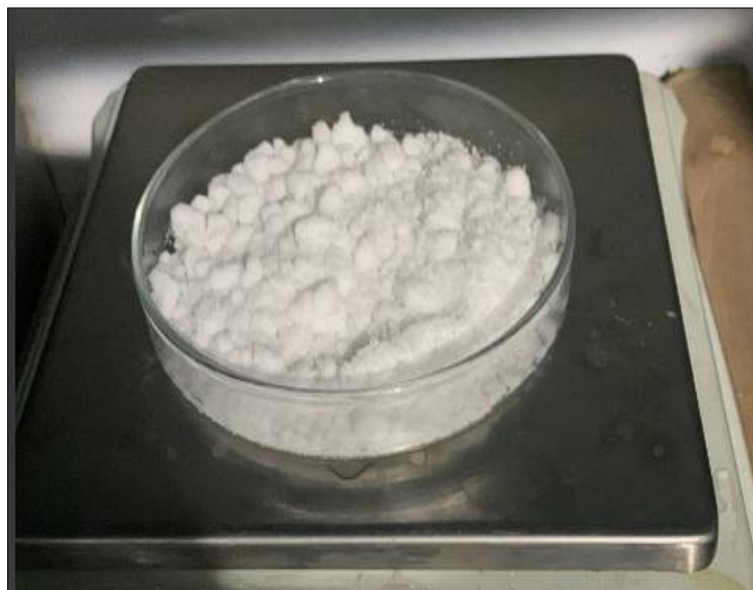


Figure 8. Reaction product at reaction temperature of 50 °C, 8 M KOH concentration, and stirring speed of 300 rpm

formation of white crystals that are identical to the K_2CO_3 available in the market. The comparison between FTIR test results in Figure 9 and the one from the K_2CO_3 standard from reference [41], as well as the comparison with wavenumbers from existing textbooks [42, 43], indicates that the product obtained in this study is K_2CO_3 (see Table 5). In Table 5, the peaks in the product from this research fall within the wavenumber range from existing references [42, 43] and are similar to pure K_2CO_3 standard [41]. The SEM test results in Figure 10 reinforce the FTIR test results from Figure

9, where the morphology of the reaction product obtained in this study (Figure 10) has characteristics identical to pure K_2CO_3 , namely having a rough and irregular surface [44] and composed of large and small particles [45]. Thus, based on the FTIR and SEM test results conducted and compared with existing references, the desired product K_2CO_3 has been formed in this reaction study. Upon further analysis, the data in Figure 11 shows that for the product amount of 54.94 grams obtained at a reaction time of 150 minutes (Figure 7), the KOH compound converted into products

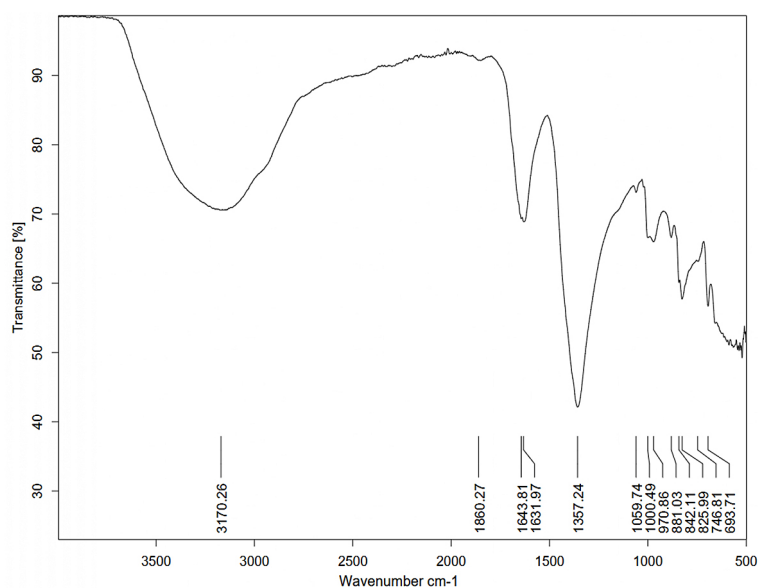


Figure 9. FTIR test results at reaction temperature of 50 °C, 8 M KOH concentration, and stirring speed of 300 rpm

Table 5. Comparison of FTIR wavenumbers from this research and standard K_2CO_3 reference [41]

Bonds	Wavenumber ranges (cm^{-1})	Standard K_2CO_3 peaks [41]	Peaks from this research	Intensity trend
O-H	3.200–3.600 [42]	3.131	3,170.26	Moderate
C=O	1.690–1.760 [42]	1.753	1,643.81	Strong
C-O	1.050–1.300 [42]	1.353	1,357.24	Strong
K-O	400–1.000 [43]	674	693.71	Strong

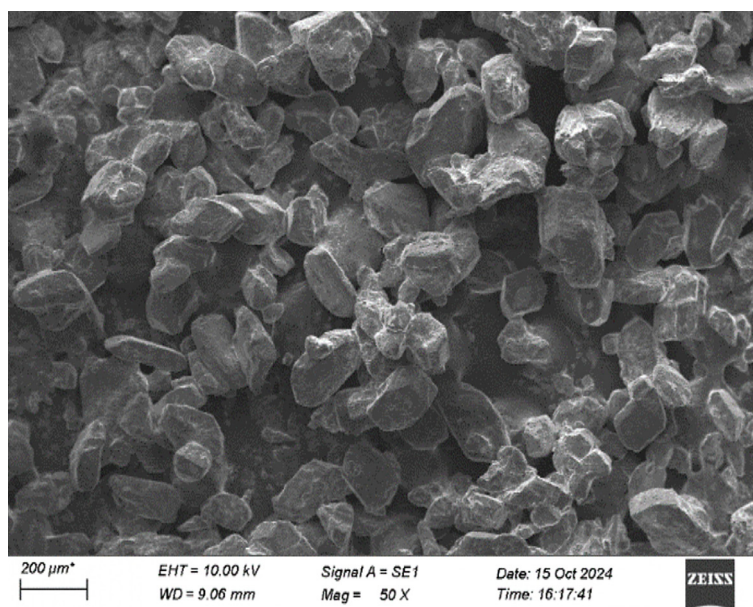


Figure 10. SEM test results at reaction temperature of 50 °C, 8 M KOH concentration, and stirring speed of 300 rpm

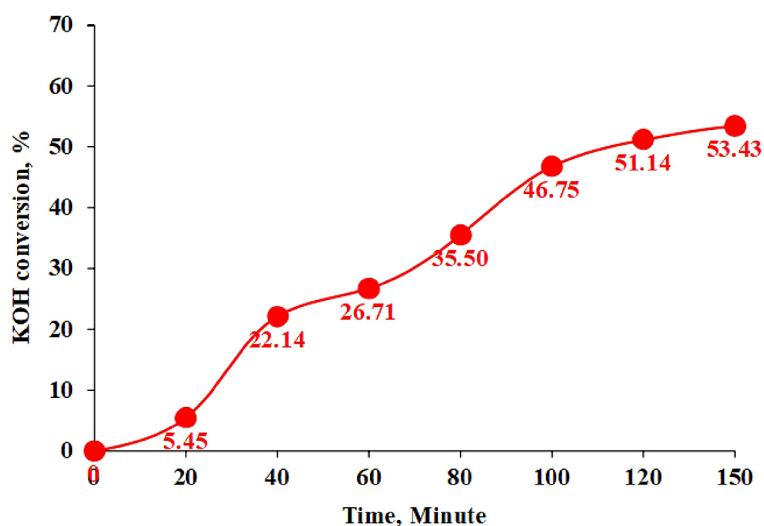


Figure 11. KOH conversion at reaction temperature of 50 °C, 8 M KOH concentration, and stirring speed of 300 rpm

(K_2CO_3 and water) was only 53.43%. This data indicates that the K_2CO_3 product can still be increased above 54.94 grams. The amount of K_2CO_3 produced can be increased using two methods: extending the reaction time beyond 150 minutes

or increasing the CO_2 inlet flow rate above 2 dm^3 per minute. Increasing the CO_2 flow rate into the reaction system above 2 dm^3 per minute is a more advantageous step, as the reduction of CO_2 will be more significant, and the amount of K_2CO_3

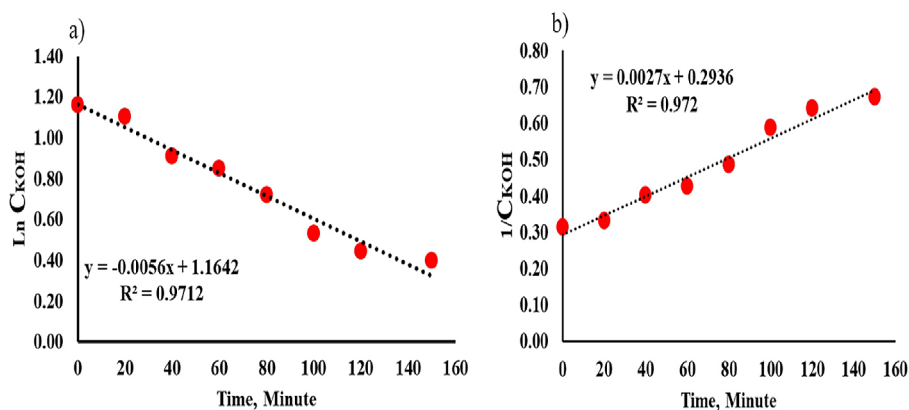
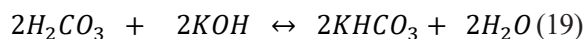
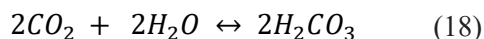


Figure 12. Mathematical model calculation results: (a) first-order, (b) second-order

produced will also be higher within the same period. However, this condition will only occur when the ratio of 1 mol CO₂ to 2 mol KOH is still maintained (see Equation (10)). However, if the reaction ratio forms a new ratio of 2 mol CO₂ to 2 mol KOH, then there is potential for KHCO₃ to form instead of K₂CO₃ (see Equation 18–19) [46]. So, when CO₂ interacts with KOH in solution, potassium bicarbonate (KHCO₃) can be produced when the stoichiometric ratio is not 1:2, meaning 1 mole of CO₂ reacts with 2 moles of KOH.



Mathematical model

In Figures 11a) and 11b, it can be seen that the R² values (determination coefficients) produced have similar values of 0.9712 (first-order) and 0.9720 (second-order). However, looking at the resulting k_1' values, the first order value is negative at -0.0056 minute⁻¹ while second-order is positive at 0.0027 dm³·mol⁻¹·minute⁻¹. Theoretically, the k_1' value cannot be negative, so it can be confirmed that this research follows the second order reaction kinetics model. The reaction rate constant (k_1') value of 0.0027 dm³·mol⁻¹·minute⁻¹ means that for each addition of 1 mol KOH, the reaction rate only increases by 0.0027 mol/ dm³ per minute. Looking at this description, the reaction between CO₂ and KOH falls into the category of slow reactions, as evidenced by the resulting conversion, which only reached 53.43% after 150 minutes (Figure 12).

CONCLUSIONS

The integration of stirring speed, KOH solution concentration, and reaction temperature positively impacted CO₂ capture, as evidenced by increased K₂CO₃ product yield. The most significant increase in K₂CO₃ was achieved when the KOH concentration parameter was increased from 4 M to 8 M, increasing by 80.30%. Overall, the best operating conditions were obtained at 8 M KOH concentration, 300 rpm stirring speed, and 50 °C reaction temperature, with a K₂CO₃ mass of 54.94 grams and KOH conversions of 53.43%. Mathematical model calculations in the form of reaction kinetics using the pseudo homogeneous approach showed that the CO₂-KOH gas reaction system follows a second-order reaction system with a k_1' value of 0.0027 dm³·mol⁻¹·minute⁻¹ with R² obtained approaching one at 0.9720. The simple process system with relatively high K₂CO₃ product mass suggests that this alternative CO₂ capture technology using a KOH solution warrants further development. Although this research has its limitations, such as the need for further observation to maximize product yields and achieve KOH conversion rates approaching 100%, the findings provide valuable insights. This study highlights how key process parameters specifically KOH concentration, system temperature, and stirring speed significantly affect the CO₂ absorption process and the resulting potassium carbonate (K₂CO₃) product. The success of this research is expected to support the development of environmentally friendly technologies for mitigating CO₂ emissions while serving as a foundation for future advancements at the pilot plant scale. As a next step, it is essential to explore how the previously studied parameters (KOH concentration, system temperature, and stirring speed)

interact with other factors, such as CO₂ gas flow rate and reaction time, over a broader range. This approach aims to maximize KOH conversion and K₂CO₃ yield. Once optimal production conditions are achieved, the subsequent step will involve refining the reactor design to align it with actual process conditions and implementing a real-time monitoring system. This refinement will enhance process control and ensure effective implementation at an industrial scale.

Acknowledgments

The authors would like to thank the Department of Chemical Engineering, Faculty of Engineering, Universitas Sultan Ageng Tirtayasa for the facilities and infrastructure provided. We hope this research will benefit the public and contribute to advancing science and technology.

REFERENCES

- Bunsen, F., Nissen, C., Hauck, J. The impact of recent climate change on the global ocean carbon sink. *Geophysical Research Letters*. 2024; 51(4): e2023GL107030. <https://doi.org/10.1029/2023GL107030>
- Bashir, A., Ali, M., Patil, S., Aljawad, M. S., Mahmoud, M., Al-Shehri, D., Kamal, M. S. Comprehensive review of CO₂ geological storage: Exploring principles, mechanisms, and prospects. *Earth-Science Reviews*. 2024; 104672. <https://doi.org/10.1016/j.earscirev.2023.104672>
- Galán, A. S. The intricate relationship between the human brain and anthropogenic global warming: impact of global warming on mental health. In *Health and Climate Change*, Academic Press. 2025; 51–71. <https://doi.org/10.1016/B978-0-443-29240-8.00005-5>
- Prajapati, M., Thesia, D., Thesia, V., Rakholia, R., Tailor, J., Patel, A., Shah, M. Carbon capture, utilization, and storage (CCUS): a critical review towards carbon neutrality in India. *Case Studies in Chemical and Environmental Engineering*. 2024; 100770. <https://doi.org/10.1016/j.cscee.2024.100770>
- Ritchie, H., & Roser, M. CO₂ emissions dataset: Our sources and methods. *Our World in Data*, 2024.
- Kakitani, K., Sugiono, W., Nakano, Y., Sato, K., Shimizu, Y. Effect of KOH and dissolved hydrogen on oxide film and stress corrosion cracking susceptibility of Alloy X-750. *Mechanical Engineering Journal*. 2024; 11(2): 23–00317. <https://doi.org/10.1299/mej.23-00317>
- Sivaramakrishnan, R., Suresh, S., Incharoensakdi, A. Development of *Chlamydomonas* sp. biorefinery for sustainable methyl ester and malic acid production. *Fuel*. 2024; 371, 132017. <https://doi.org/10.1016/j.fuel.2024.132017>
- Picard, K., Picard, C., Mager, D. R., Richard, C. Potassium content of the American food supply and implications for the management of hyperkalemia in dialysis: an analysis of the Branded Product Database. In *Seminars in Dialysis*. 2024; 37(4): 307–316. <https://doi.org/10.1111/sdi.13007>
- Shojaee Barjoe, S., & Rodionov Alekseevich, V. Respirable Dust in Ceramic Industries (Iran) and its Health Risk Assessment using Deterministic and Probabilistic Approaches. *Pollution*. 2024; 10(4), 1206–1226. <https://doi.org/10.22059/poll.2024.376043.2360>
- Mourad, A. A., Mohammad, A. F., Al-Marzouqi, A. H. Evaluation of bovine carbonic anhydrase for promoting CO₂ capture via reaction with KOH and high-salinity reject brine. *Journal of CO₂ Utilization*. 2024; 81, 102714. <https://doi.org/10.1016/j.jcou.2024.102714>
- Rivera, R. M., Binnemans, K. Carbon dioxide as a sustainable reagent in circular hydrometallurgy. *ChemSusChem*. 2024; e202400931. <https://doi.org/10.1002/cssc.202400931>
- Saeidi, M., Ghaemi, A., Tahvildari, K. CO₂ capture exploration on potassium hydroxide employing response surface methodology, isotherm and kinetic models. *Iranian Journal of Chemistry and Chemical Engineering (IJCCE)*. 2020; 39(5), 255–267.
- Smith, J. M., Van Ness, H. C., Abbott, M. M., Swihart, M. T. *Introduction to chemical engineering thermodynamics*. 8th edition. Singapore: McGraw-Hill. 2018.
- Yao, C., Dong, Z., Zhao, Y., Chen, G. Gas-liquid flow and mass transfer in a microchannel under elevated pressures. *Chemical Engineering Science*. 2015; 123, 137–145. <https://doi.org/10.1016/j.ces.2014.11.005>
- Singh, J., Bhunia, H., Basu, S. Adsorption of CO₂ on KOH activated carbon adsorbents: Effect of different mass ratios. *Journal of environmental management*. 2019; 250, 109457. <https://doi.org/10.1016/j.jenvman.2019.109457>
- Firman, N. F. A., Noor, A., Zakir, M., Maming, M., Fathurrahman, A. F. Absorption of carbon dioxide into potassium hydroxide: Preliminary study for its application into liquid scintillation counting procedure. *Egyptian Journal of Chemistry*. 2021; 64(9): 4907–4912. <https://dx.doi.org/10.21608/ejchem.2021.66304.3506>
- Mourad, A. A., Mohammad, A. F., Al-Marzouqi, A. H., Altarawneh, M., Al-Marzouqi, M. H., El-Naas, M. H. Carbon dioxide capture through reaction with potassium hydroxide and reject brine:

- A kinetics study. *International Journal of Greenhouse Gas Control*. 2022; 120, 103768. <https://doi.org/10.1016/j.ijggc.2022.103768>
18. Rastegar, Z., Ghaemi, A. CO₂ absorption into potassium hydroxide aqueous solution: experimental and modeling. *Heat and Mass Transfer*. 2022; 58(3), 365–381. <https://doi.org/10.1007/s00231-021-03115-9>
 19. Li, D., Yan, B., Gao, T., Li, G., Wang, Y. PINN Model of Diffusion Coefficient Identification Problem in Fick's Laws. *ACS omega*. 2024; 9(3), 3846–3857. <https://doi.org/10.1021/acsomega.3c07924>
 20. Zhu, H., Lei, Y., Yu, P., Li, C., Yao, B., Yang, S., Peng, H. Novel high-precision wax molecular diffusion coefficient correlation based on the diffusion laboratory apparatus coupled with differential scanning calorimeter. *Fuel*. 2024; 355, 129452. <https://doi.org/10.1016/j.fuel.2023.129452>
 21. Jabalquinto, A. R., Mai, N., Belghiche, S., Gill, P. P. Modified Arrhenius kinetics for double base propellant decomposition: effect of water. *Polymer Degradation and Stability*. 2024; 110846. <https://doi.org/10.1016/j.polymdegradstab.2024.110846>
 22. Brettfeld, E. G., Popa, D. G., Dobre, T., Moga, C. I., Constantinescu-Aruxandei, D., Oancea, F. CO₂ Capture Using Deep Eutectic Solvents Integrated with Microalgal Fixation. *Clean Technologies*. 2023; 6(1): 32-48. <https://doi.org/10.3390/cleantechnol6010003>
 23. Nuryoto N., Heriyanto H, Rahmawati L., Herliza J. Greenhouse Gas Transformation: Converting CO₂ into High-Value Material as Precipitated Calcium Carbonate (PCC) (original title: Transformasi Gas Rumah Kaca: Mengubah CO₂ Menjadi Bahan Bernilai Tinggi Berupa Precipitated Calcium Carbonate (PCC)). *Jurnal Sains & Teknologi*. 2024; 13(2). <https://doi.org/10.23887/jstundiksha.v13i2.79553>
 24. Moreno, V. C., Ledoux, A., Estel, L., Derrouiche, S., Denieul, M. P. Valorisation of CO₂ with epoxides: Influence of gas/liquid mass transfer on reaction kinetics. *Chemical Engineering Science*. 2017; 170, 77–90. <https://doi.org/10.1016/j.ces.2017.01.050>
 25. Kierzkowska-Pawlak, H. Determination of kinetics in gas-liquid reaction systems. An overview. *Ecological Chemistry and Engineering S*. 2012; 19(2), 175–196. <https://doi.org/10.2478/v10216-011-0014-y>
 26. Wanten, B., Gorbanev, Y., Bogaerts, A. Plasma-based conversion of CO₂ and CH₄ into syngas: A dive into the effect of adding water. *Fuel*. 2024; 374, 132355. <https://doi.org/10.1016/j.fuel.2024.132355>
 27. Adu, E., Zhang, Y. D., Liu, D., Tontiwachwuthikul, P. Parametric process design and economic analysis of post-combustion CO₂ capture and compression for coal-and natural gas-fired power plants. *Energies*. 2020; 13(10), 2519. <https://doi.org/10.3390/en13102519>
 28. Abdullah, N. T., Shakir, I. K. Efficient carbon dioxide capture in packed columns by solvents blend promoted by chemical additives. *Journal of Ecological Engineering*. 2024; 25(10). <https://doi.org/10.12911/22998993/191436>
 29. Atmani, F., Kaci, M. M., Yeddou-Mezenner, N., Soukeur, A., Akkari, I., Navio, J. A. Insights into the physicochemical properties of Sugar Scum as a sustainable biosorbent derived from sugar refinery waste for efficient cationic dye removal. *Biomass Conversion and Biorefinery*. 2024; 14(4), 4843–4857. <https://doi.org/10.1007/s13399-022-02646-3>
 30. Kosolapova, S. M., Smal, M. S., Pyagay, I. N., Rudko, V. A. The Physicochemical basis for the production of rapeseed oil fatty acid esters in a plug flow reactor. *Processes*. 2024; 12(4), 788. <https://doi.org/10.3390/pr12040788>
 31. Zhao, B., Li, H., Liu, Q., Su, Y. Modeling and simulation of gas vortex flow dynamics to understand the nature of mass transfer enhancement. *Physics of Fluids*. 2023; 35(6). <https://doi.org/10.1063/5.0156468>
 32. Shi, S., Wu, X., Han, G., Zhong, Z. Study on the gas-liquid annular vortex flow for liquid unloading of gas well. *Oil & Gas Science and Technology-Revue d'IFP Energies Nouvelles*. 2019; 74, 82. <https://doi.org/10.2516/ogst/2019052>
 33. Ouyang, Y., Manzano, M. N., Beirnaert, K., Heyndrickx, G. J., & Van Geem, K. M. (Micromixing in a gas-liquid vortex reactor. *AIChE Journal*. 2021; 67(7): e17264. <https://doi.org/10.1002/aic.17264>
 34. Omranpour, S., Larimi, A. Modeling and simulation of biodiesel synthesis in fixed bed and packed bed membrane reactors using heterogeneous catalyst: a comparative study. *Scientific Reports*. 2024; 14(1): 10153. <https://doi.org/10.1038/s41598-024-60757-5>
 35. Joel, A. S., Wang, M., Ramshaw, C., Oko, E. Process analysis of intensified absorber for post-combustion CO₂ capture through modelling and simulation. *International Journal of Greenhouse Gas Control*. 2014; 21, 91–100. <https://doi.org/10.1016/j.ijggc.2013.12.005>
 36. Yuan, B., Zhan, G., Xing, L., Li, Y., Huang, Z., Chen, Z., Li, J. Boosting CO₂ absorption and desorption of biphasic solvent by nanoparticles for efficient carbon dioxide capture. *Separation and Purification Technology*. 2024; 329, 125108. <https://doi.org/10.1016/j.seppur.2023.125108>
 37. Chabab, S., Kerkache, H., Bouchkira, I., Poulain, M., Baudouin, O., Moine, É., Cézac, P. Solubility of H₂ in water and NaCl brine under subsurface storage conditions: Measurements and thermodynamic modeling. *International Journal of Hydrogen Energy*. 2024; 50, 648–658. <https://doi.org/10.1016/j.ijhydene.2023.10.290>
 38. Wang, Z., Christodoulou, C., Mazzei, L. Analytical

- study on the liquid-particle mass transfer coefficient for multiparticle systems. *Chemical Engineering Journal*. 2024; 152733. <https://doi.org/10.1016/j.cej.2024.152733>
39. Maluta, F., Alberini, F., Paglianti, A., Montante, G. A CFD study on the change of scale of non-Newtonian stirred digesters at low Reynolds numbers. *Chemical Engineering Research and Design*. 2024; 205, 498–509. <https://doi.org/10.1016/j.cherd.2024.04.018>
40. Chen, T. Y., Ho, W. W. Effects of pressure and temperature on CO₂ facilitation of amino acid salt-containing membranes for post-combustion carbon capture. *Journal of Membrane Science*. 2024; 689, 122166. <https://doi.org/10.1016/j.memsci.2023.122166>
41. Institute of Chemistry University of Tartu. Data Base of ATR-FTIR Spectra of various materials-Potassium Carbonate. Potassium Carbonate – Database of ATR-FT-IR spectra of various materials, , 2024 (accessed on 28 December 2024).
42. Skoog, D., Holler, T., Nieman, F. Principles of Instrumental Analysis. 5th edition. Philadelphia: Saunders College Pub.; Orlando, Fla.: Harcourt Brace College Publishers. 1998.
43. Stuart, B. Infrared Spectroscopy Fundamental and Applications. John Wiley & Sons Ltd. New York. 2004.
44. Lin, J., Zhao, Q., & Huang, H. Performance Analysis of Vermiculite–Potassium Carbonate Composite Materials for Efficient Thermochemical Energy Storage. *Energies*. 2024; 7(12): 2847. <https://doi.org/10.3390/en17122847>
45. Masoud, N., Clement, V., van Haasterecht, T., Führer, M., Hofmann, J. P., Bitter, J. H. Shedding Light on Solid Sorbents: Evaluation of Supported Potassium Carbonate Particle Size and Its Effect on CO₂ Capture from Air. *Industrial & Engineering Chemistry Research*. 2022; 61(38), 14211–14221. <https://doi.org/10.1021/acs.iecr.2c01508>
46. Liu, G. H., Deng, L. T., Wen, M. M., Cui, H. N., Huang, J. Y., Wang, C. F., Chen, T. R. Determination of concentration of free carbon dioxide in artificial seawater by difference balance system/Henry's law. *Sustainability*. 2023; 15(6), 5096. <https://doi.org/10.3390/su15065096>